

# Preprocessing noisy functional data using factor models

Siegfried Hörmann\*

Institute of Statistics, Graz University of Technology  
and

Fatima Jammoul

Institute of Statistics, Graz University of Technology

December 11, 2020

## Abstract

We consider functional data which are measured on a discrete set of observation points. Often such data are measured with noise, and then the target is to recover the underlying signal. Most commonly, practitioners use some smoothing approach, e.g., kernel smoothing or spline fitting towards this goal. The drawback of such curve fitting techniques is that they act function by function, and don't take into account information from the entire sample. In this paper we argue that signal and noise can be naturally represented as the common and idiosyncratic component, respectively, of a factor model. Accordingly, we propose to an estimation scheme which is based on factor models. The purpose of this paper is to explain the reasoning behind our approach and to compare its performance on simulated and on real data to competing methods.

*Keywords:* functional data, factor models, preprocessing, signal-plus-noise

---

\*Corresponding author. Email: shoermann@tugraz.at

# 1 Introduction

Functional data analysis (FDA) is concerned with the analysis of data that can naturally be described as curves. In mathematical terms data are modeled as random curves  $(X(s): s \in \mathcal{S})$ , where  $\mathcal{S}$  is some continuum. Examples where such data arise are very diverse, ranging from high frequency asset price curves, over growth curves or pollution level curves, to 2D satellite images or fMRI scans. For a simple presentation we assume without loss of generality that  $\mathcal{S} = [0, 1]$ . With technological advances recording and storing this type of data becomes more and more common and hence the corresponding FDA literature has seen a big upsurge over the past years. For an introduction to the topic we refer, for example, to the textbooks of Horváth and Kokoszka (2012) or Ramsay and Silverman (2005).

In practice functional data are not fully observed, but sampled on a discrete set of time points. Consider functional observations  $(X_t(s): 0 \leq s \leq 1)$ ,  $t \geq 1$ , and assume we have measurements of it at time points  $0 \leq s_1 < s_2 < \dots < s_p \leq 1$ . A very common working hypothesis in FDA literature is that these measurements come with an additional error, so that we actually observe

$$y_t = (X_t(s_1), \dots, X_t(s_p))' + (u_{t1}, \dots, u_{tp})' =: X_t(\mathbf{s}) + u_t. \quad (1.1)$$

(Henceforth we are going to write  $\mathbf{s}$  for  $(s_1, \dots, s_p)$  and use the convention that  $g(\mathbf{s})$  denotes  $(g(s_1), \dots, g(s_p))'$ .) The errors  $u_t$  can, for example, be related to measurement errors, and the goal is to separate those from  $X(\mathbf{s})$ . Most papers (e.g., those cited below) assume that the components  $(u_{ti}: 1 \leq i \leq p)$  are i.i.d. with zero mean and variance  $\sigma_u^2 > 0$  and that  $X_t$  and  $u_t$  are independent. To recover  $X_t$  (henceforth we call it the *signal*) a variety of fitting techniques exist, which lead to a fitted curve  $\hat{X}_t$ . Obviously, the goal is to acquire an estimate  $\hat{X}(\mathbf{s})$  that is close to the latent signal  $X(\mathbf{s})$ . A very common technique is the basis expansion approach, explained thoroughly in Ramsay and Silverman (2005). Here, the fitted curve is a linear combination of suitable basis functions. Most popular choices are the Fourier basis or B-splines. By adding a roughness penalty to the least squares criterion the smoothness of the curves can be controlled. Other approaches employ kernel smoothing (see e.g., Ramsay and Silverman (2005); Stadtmüller and Zampiceni (2015)), with a detailed description in Wand and Jones (1995), where a kernel function is used to estimate the signal. Most prominent is the Nadaraya-Watson regression estimate as proposed in Nadaraya (1964) and Watson (1964).

Nevertheless, the recovery of the true signal remains a delicate problem when analysing real data. The degree of smoothness of the signal, which is needed to choose the appropriate number of basis functions or the bandwidth of a kernel smoother, is typically unknown and then the result of the analysis is influenced by a non-verifiable working hypothesis. Cross-validation (CV) may look like an attractive route, since there the parameter choices become data driven. To illustrate that the problem is still challenging, look at the synthetic example in Figure 1. The two rows in the graph illustrate realisations from two random samples (four observations each). The dots represent the raw data  $y$  and the green lines the underlying signals  $X(s)$ . In the first example (top row) the data generating process (DGP) is such that all intraday data have a higher variability

at  $s = 0.7$ , while in the second example (bottom row) the actual data form straight lines with one outlying measurement error in the second observation. With curve-by-curve fitting techniques, it is not possible to distinguish between a measurement error or some systematic structure in the signal. We would need further measurements in the neighbourhood of  $s = 0.7$ , where the signal is erratic. So the accuracy in recovering the signal is tied to its smoothness, and the relevant question is whether  $p$  is large enough relative to the degree of smoothness to sufficiently justify a certain approach.

Suppose now that we want to estimate the signals for a sample  $y_1, \dots, y_T$ . While  $p \rightarrow \infty$  is favourable for curve-by-curve fitting techniques, i.e., when  $\hat{X}_t = \mathcal{F}_t(y_t)$  for some operator  $\mathcal{F}_t$ , say, *no improvement in the fit can be expected if we let  $T$  grow*. This suggests employing a fitting procedure which takes into account the entire sample, i.e.,  $\hat{X}_t = \mathcal{G}_t(y_1, \dots, y_T)$ . Staniswalis and Lee (1998) proposed a method of this type. Under

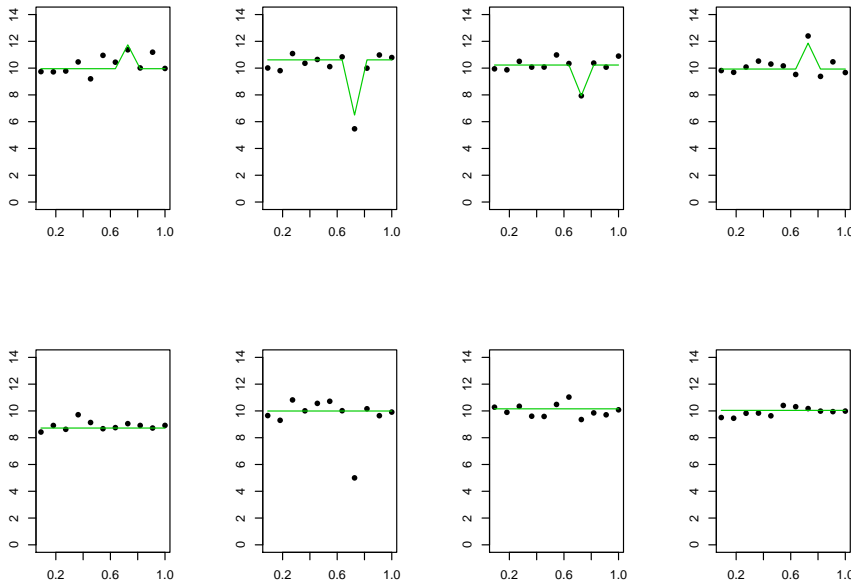


Figure 1: In this illustrative example, the dots correspond to measurements  $y$  and the green solid lines to the actual signals  $X(s)$ .

model (1.1), say with iid errors, we have that  $\text{Var}(y) = \text{Var}(X(\mathbf{s})) + \sigma^2 I_p$  (with  $I_p$  being the identity matrix in  $\mathbb{R}^{p \times p}$ ). Hence,

$$((\widehat{\text{Var}}(y)))_{k,k'} = \frac{1}{T} \sum_{t=1}^N (y_{tk} - \bar{y}_{\cdot k})(y_{tk'} - \bar{y}_{\cdot k'}) \approx \text{Cov}(X(s_k), X(s_{k'})) + \sigma^2 I\{s_k = s_{k'}\},$$

where  $y_{tk}$  is the  $k$ -th component of  $y_t$  and  $\bar{y}_{\cdot k} = \frac{1}{T} \sum_{t=1}^T y_{tk}$ . Their idea is to estimate the covariance kernel  $\text{Cov}(X(s), X(s'))$  by smoothing the  $p \times p$  matrix  $\text{Var}(y)$ . The smoothing step is used to remove the discontinuity on the diagonal, which is due to the noise  $u$ .

They propose a kernel smoother, but other approaches such as spline smoothing can be used instead. Denote the smooth covariance kernel estimator by  $\widehat{\text{Cov}}(X(s), X(s'))$ .

In a second step the estimated eigenfunctions  $\hat{\psi}_i$  of  $\widehat{\text{Cov}}(X(s), X(s'))$ , which form an orthonormal basis, are used to expand the  $X_t$  along this basis. The resulting expansion provides an estimator of the signal. For further details we refer to the original paper.

Several subsequent articles are based on variants of this approach. For example, the well known PACE algorithm established in Yao et al. (2005) makes use of the idea described above. Other important references focus on the estimation of eigenfunctions and eigenvalues from the smoothed covariance and derive asymptotic results. We refer in particular to Hall et al. (2006) and Müller et al. (2006).

In our paper we would like to complement the literature with an additional route. The main difference to existing methods is that we do not pursue the idea of smoothing, but keep the model (like the actual measurements) multivariate. *We focus on the high dimensional setups ( $p \rightarrow \infty$ ), where the number of observed curves is large as well ( $T \rightarrow \infty$ ).* We show in the next section that functional data sampled as in (1.1) follow some *factor model*. The signal underlying the observations is related to the *common components* in a factor model and thus our strategy is to estimate these common components. In this way, our method doesn't rely on particular smoothness conditions of the signal.

The rest of the paper is organised as follows. In Sections 2.1 and 2.2 we outline the main idea behind our approach. In Section 2.3 we discuss simple diagnostic tools which may help to practically assess the quality of signal estimation. Then, for the convenience of the reader we give a short survey of factor models in Section 2.4. Section 3 is concerned with a PCA based estimation scheme for the factor model. In Section 4 we provide comprehensive simulation studies. For this purpose we create synthetic samples out of PM10 (particular matter) data, which allows us to have a controllable and at the same time realistic data base, as seen in Section 4.1. In order to demonstrate that our method doesn't require specific smoothness conditions, we provide an additional simulation study considering signals which may contain a discontinuity in Section 4.2. In Section 5 we analyse and compare two real data sets of Canadian temperature data. We conclude in Section 6.

## 2 Basic idea of our method

We consider a sample of functional data  $X_1, \dots, X_T$  defined on a common probability space. Throughout we assume that observations are i.i.d. or form a general stationary functional process. The curves  $(X_t(s) : s \in [0, 1])$  are square integrable on  $[0, 1]$ , and hence can be expanded along a sequence of orthogonal basis functions  $\{b_k(s) : k \geq 1\}$ , (for example the Fourier basis). Then we have  $X_t(s) = \sum_{k \geq 1} \langle X_t, b_k \rangle b_k(s)$ , where  $\langle a, b \rangle = \int_0^1 a(v)b(v)dv$ . We assume for our presentation that the curves have a finite dimension, i.e., that

$$X_t(s) = \sum_{k=1}^L \langle X_t, b_k \rangle b_k(s), \quad \text{for some } L \geq 1. \quad (2.2)$$

Otherwise, (2.2) holds approximately if  $L$  is big enough. When choosing a suitable basis (e.g., functional principal components) a good approximation typically only requires small to moderate sized values of  $L$ .

A basic requirement for our proposed method is that all curves are sampled at time points  $0 \leq s_1 < s_2 < \dots < s_p \leq 1$ . This is a very common setting for machine recorded data. We note that sampling points need not be equidistant though. We will assume throughout a general signal-plus-noise structure as in (1.1).

## 2.1 Representation in factor model form

Our method is based on the following representation theorem for functional data observed as in (1.1).

**Proposition 2.1.** *Suppose (1.1) and (2.2) hold. Let  $u_t$  be independent of  $X_t$  and assume that  $Eu_t = 0$  and  $\text{Var}(u_t) = \text{diag}$ . Then  $y_t$  follows a  $L$ -factor model.*

*Proof.* We show that there exists a matrix  $B \in \mathbb{R}^{p \times L}$  such that

$$y_t = \mu(\mathbf{s}) + Bf_t + u_t, \quad (2.3)$$

where  $\mu(s) = EX_t(s)$ ,  $Ef_t = 0$ ,  $\text{Var}(f_t) = I_L$  (the identity matrix in  $\mathbb{R}^L$ ) and  $\text{Cov}(f_t, r_t) = 0$ .

We denote the covariance function of  $X_t$  by  $\Gamma^X(s, s') = \text{Cov}(X_t(s), X_t(s'))$ . Since we assume stationarity, this covariance kernel doesn't depend on  $t$ . Using (2.2) the Karhunen-Loève expansion gives

$$X_t(s) = \mu(s) + \sum_{\ell=1}^L x_{t\ell} \varphi_\ell(s), \quad (2.4)$$

where  $\varphi_\ell(s)$  are the eigenfunctions of the covariance operator  $\Gamma^X$  and  $x_{t\ell} = \int_0^1 (X_t(s) - \mu(s)) \varphi_\ell(s) ds$ . The scores ( $x_{t\ell}$ :  $\ell \geq 1$ ) are uncorrelated and  $\text{Var}(x_{t\ell}) = \lambda_\ell$ , where  $\lambda_\ell$  are the eigenvalues of  $\Gamma^X$  (in decreasing order). See e.g., Bosq (2000) for details. Define now the matrix  $B := (\sqrt{\lambda_1} \varphi_1(\mathbf{s}), \dots, \sqrt{\lambda_L} \varphi_L(\mathbf{s}))$ . Moreover, define  $f_t = (x_{t1}/\sqrt{\lambda_1}, \dots, x_{tL}/\sqrt{\lambda_L})'$ . This yields the desired representation.  $\square$

In factor model language  $Bf_t$  are called the *common components* of  $y_t$  and our problem is reduced to the estimation of these common components—we expand on this in the next section. Let us conclude here with a very important observation: It is common in FDA to also smooth data, which by their very nature come without relevant measurement errors (e.g., annual temperature curves generated from daily data, intraday stock prices, etc.) In this case it needs to be clarified how the residual noise is to be interpreted. The translation of our problem into factor model language gives a mathematical/statistical meaning to the noise  $u_t$  which goes beyond measurement errors. The  $u_t$  define the *idiosyncratic components* of  $y_t$ , which are characterised by being uncorrelated or, more generally, be weakly correlated in a certain sense to be specified. The components of  $u_t$  represent “unsystematic” fluctuations in our functional trajectories.

## 2.2 General estimation approach

As it was mentioned above, the signal  $X(\mathbf{s})$  is related to the common components of  $y_t$ . The core idea of the algorithm that we pursue is simple and can be summarised as follows:

### Core algorithm:

1. Estimate  $\mu(\mathbf{s})$  by  $\hat{\mu}(\mathbf{s}) = \frac{1}{T}(y_1 + \dots + y_T)$ .
2. Center the data by  $\hat{\mu}(\mathbf{s})$ .
3. Choose an appropriate order  $L$ .
4. Approximate  $X_t(\mathbf{s}) - \mu(\mathbf{s})$  through the estimated *common components*:  $\hat{B}\hat{f}_t$ .
5. Set  $\hat{X}_t(\mathbf{s}) = \hat{\mu}(\mathbf{s}) + \hat{B}\hat{f}_t$ .

Steps 3. and 4. can be carried out by many existing approaches for estimating factor models. For convenience of readers who are less familiar with the corresponding literature, a short survey is given below in Section 2.4. In applications the user is free to choose any estimation method leading to satisfactory and plausible results. (See Section 2.3.)

**Remark 1.** *A known problem in factor model theory is that factor loadings and the factor scores are not unique. If  $O \in \mathbb{R}^L$  is some orthogonal matrix, then  $Bf = (BO)(O'f)$ , and  $\text{Var}(O'f) = I_L$ . This identification issue is not a problem here, because we are primarily interested in the common components  $Bf$ , which remain well identified.*

**Remark 2.** *The factor approach doesn't return a full curve, but an estimate of the noise-free curves at the points  $0 \leq s_1 < s_2 < \dots < s_p \leq 1$ . If the goal is to work with full curves, then it is up to the experimenter to choose a discrete-to-function transformation, which is designated for noise-free data. However, it should be noted that for functional data, which are not given in a basis function representation, the processing requires discretisations anyway (e.g., when calculating eigenfunctions or computing inner products). In this case continuous time estimates are not needed.*

## 2.3 Model diagnostics

A simple diagnostic tool which may help to discern inadequate signal extraction is the inspection of the covariance of the residuals. Consider the fits  $\hat{X}_1(\mathbf{s}), \dots, \hat{X}_T(\mathbf{s})$  and denote by  $\hat{u}_t = y_t - \hat{x}_t$  the residual vectors (here  $\hat{x}_t = (\hat{X}_t(s_1), \dots, \hat{X}_t(s_p))'$ ). Each residual vector  $\hat{u}_t$  defines a time series  $\hat{u}_{t1}, \dots, \hat{u}_{tp}$ . For example, if  $(u_{ti}: 1 \leq i \leq p)$  is assumed to be white noise, then this should be reflected in the empirical autocorrelation functions (acf's)

$$\hat{\gamma}_{\hat{u}_t}(h) = \frac{1}{p} \sum_{t=1}^{p-|h|} (\hat{u}_{t(i+h)} - \bar{\hat{u}}_t)(\hat{u}_{ti} - \bar{\hat{u}}_t). \quad (2.5)$$

Since we have replicates, we may also conclude that

$$\hat{\Gamma}^{\hat{u}} := \frac{1}{T} \sum_{t=1}^T (\hat{u}_t - \bar{\hat{u}})(\hat{u}_t - \bar{\hat{u}})' \approx \text{Var}(u), \quad (2.6)$$

where  $\bar{\hat{u}}$  is the grand mean of  $\hat{u}_1, \dots, \hat{u}_T$ . If there is doubt that the noise components are stationary (e.g., if the homogeneous variance assumption is likely to be violated) analysing  $\hat{\Gamma}^{\hat{u}}$  may be preferable over investigating the acf's  $\hat{\gamma}_{\hat{u}_t}$ .

If (2.6) doesn't hold, this indicates that the transformation from discrete to functional data introduced some bias. In our real data examples (Section 5) we investigate daily temperatures and corresponding annual temperature curves from Canada. Following Ramsay et al. (2009), the daily data were transformed with 65 Fourier basis functions and a roughness penalty to annual curves. In Figure 2 we show the acf's (2.5) of the residual vectors at a station in Montreal in the years 1961, 1978 and 1993. We also show the heat map representing the righthand side in (2.6). For better visibility, the heat map is restricted to the first 2 months of the year. Details on the data and the

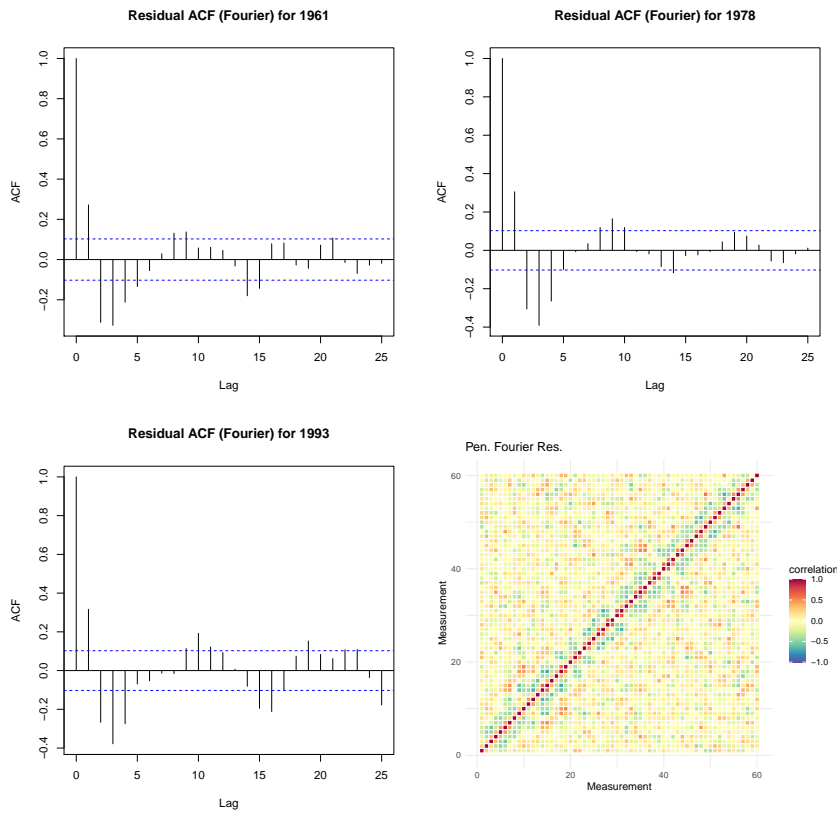


Figure 2: Autocorrelation function of residual vectors for the *Montreal Weather Data* for the years 1961, 1978, 1993 and the heat map corresponding to the lefthand side in (2.6).

implementation will be given in Section 5. At this stage, we want to draw the readers attention to the spurious oscillation in the acf's. If the components of the error vectors were iid—as it is commonly assumed—then the acf should be zero for all lags  $\neq 0$ . In a slightly more realistic setting we would expect some moderate positive correlation of the errors, which tapers to zero with increasing lag. The same observation is made if we replace the Fourier basis with 65 B-splines, implying that the oscillation is not an

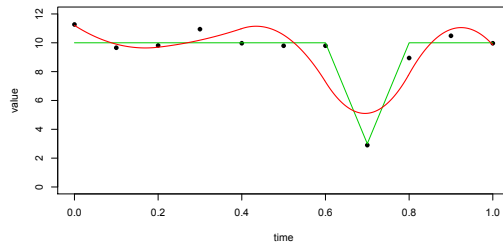


Figure 3: The green curve corresponds to  $X(s)$ . The red curve is a B-spline fit and the black dots correspond to actual observations.

artefact stemming from the Fourier functions. An explanation for this phenomenon can be deduced from our synthetic example. As is illustrated in Figure 3, the basis functions fit has the tendency to compensate underestimation of the signal at one time point with overestimation at the subsequent time point(s). This is particularly pronounced at the spiky peak.

## 2.4 Some background on factor models

There is an extensive literature on factor models. In this section we list a few papers which appear most relevant in our context and which address data where both the cross-sectional and the temporal dimension is large. As we have mentioned in the introduction, we are particularly interested in settings where  $p$  and  $T$  are large. These models have proven to be particularly useful in econometric applications for markets with many assets. For example, they can be used to forecast high-dimensional panel data (Stock and Watson (2002a,b)). Forecasting requires modeling time dependence and here a fundamental framework is provided by so-called generalized dynamic factor models (Forni and Lippi (2001)). In the context of such macroeconomic applications, Chamberlain and Rothschild (1983) have shown that it is useful to allow also for a certain degree of dependence in the idiosyncratic noise. It is then referred to *approximate factor models*. All these features are natural and useful in our context, too: (1) The dimension  $p$  of our sampling points  $\mathbf{s}$  is large and allowed to diverge with increasing sample size. (2) The functional data  $X_t$  may be time-dependent, i.e., form a functional time series. (3) In a realistic framework, measurement errors ( $u_{ti}$ ) in (1.1) might be correlated at small lags.

Next to conceptual papers dealing with the questions of how to define and use different variants of factor models in diverse applications, there is also a profound literature on estimation theory for these models. In particular we refer to the papers of Bai (2003), Bai and Li (2012), Choi (2012) and Bai and Liao (2016), Fan et al. (2013) and Bai and Li (2016). In context of dynamic factor models we refer to Forni et al. (2000, 2005).

There are two common approaches for factor model estimation. One strategy is to utilize principal component analysis, e.g., Chamberlain and Rothschild (1983) use this method. PCA is particularly simple to implement and doesn't require numerically intense stochastic optimization methods. Bai (2003) investigated the asymptotic behaviour of

both the factors as well as the factor loadings and—under technical conditions—proved consistency as well as robustness to mild correlation in the error terms.

The second popular strand is based on maximum likelihood. Choi (2012) expanded upon previous ideas by describing an efficient estimation for factor models, where the conditional distribution of  $u_t|f_1, \dots, f_T$  is assumed to be normal with a covariance matrix that is not necessarily diagonal. Bai and Li (2012, 2016) provide a method involving a quasi-maximum-likelihood approach where the factors  $f_t$  are regarded as fixed constants. We refer to Anderson (2003) for details about the derivation of the likelihood.

Let us mention that in many of the above listed papers, the number of factors  $L$  is fixed and assumed to be a known entity. This, of course, is not a realistic assumption and in practice  $L$  needs to be estimated. Bai and Ng (2002) is a key reference for this problem. Hallin and Liška (2007) expanded the approach to dynamic factor models. Onatski (2010) proposes an approach that uses the empirical distribution (ED) of the eigenvalues of the sample covariance matrix. Owen and Wang (2016) use a Bi-Cross-Validation (BCV) technique to estimate the number of factors. Contrary to other approaches, they're not specifically interested in recovering the true number of factors, but rather the number of factors best-suited to recover the underlying signal. In the process of our empirical work, we have investigated the behaviour of these estimators. We found that the BCV and ED worked best in our FDA context. Other approaches we explored seemed to underestimate the number of factors severely for our purposes.

### 3 A PCA approach for estimating the signal

In general both the PCA or MLE approach can be used in our context. We focus on the PCA approach, because it is very easy to implement and gave slightly better results in our simulation study.

We assume henceforth that the data are already centred, i.e., step one in our algorithm has already been carried out. The estimator we are considering is then of the form

$$(\hat{X}_1(\mathbf{s}), \dots, \hat{X}_T(\mathbf{s})) = Y \hat{E} \hat{E}', \quad (3.7)$$

where  $Y = (y_1, \dots, y_T)$  and where  $\hat{E} = (\hat{e}_1, \dots, \hat{e}_L)$  are the eigenvectors of  $\frac{1}{T} Y' Y$  associated to the  $L$  largest eigenvalues  $\hat{\gamma}_1 \geq \dots \geq \hat{\gamma}_L$ . To explain how this estimate is motivated, let us elaborate on some further notation related to the factor model setting. We define  $U = (u_1, \dots, u_T)$  and  $F' = (f_1, \dots, f_T)$ . Moreover, we let  $b'_j$  be the  $j$ -th row of  $B$ . The  $j$ -th column of  $Y'$  and  $U'$  are denoted  $Y_j$  and  $U_j$ , respectively. The  $j$ -th row of  $F'$  is denoted by  $F_j$ . Then we can write our model equation (2.3) in the compact matrix form

$$Y = B F' + U. \quad (3.8)$$

In this notation, the objective is to estimate  $B F'$  through some estimator  $\hat{B} \hat{F}'$ .

Suppose that  $F$  is already known. Then  $Y_j = F b_j + U_j$ , which leads to the common least-squares estimator  $\hat{b}_j^{\text{LS}} = (F' F)^{-1} F' Y_j$ . If our data are independent (or satisfy some appropriate weak dependence condition), we get by the law of large numbers and

orthogonality of principal components scores that

$$\frac{1}{T}F'F \xrightarrow{P} I_L. \quad (3.9)$$

This motivates  $\hat{B}_{|F} := \frac{1}{T}YF$  as estimator for  $B$  conditional on  $F$ . For  $F$  in turn we use the empirical principal components and set  $\hat{F} = \sqrt{T}\hat{E}$ . Then  $\frac{1}{T}\hat{F}'\hat{F} = I_L$ . In summary  $\hat{F} = \sqrt{T}\hat{E}$  and  $\hat{B} = \frac{1}{T}Y\hat{F}$ , which implies that  $\widehat{BF}' := \hat{B}\hat{F}' = Y\hat{E}\hat{E}'$ .

From a theoretical perspective it is interesting to give technical conditions needed for establishing consistency results. However, it is not straight forward to translate existing theorems on factor models into a functional data setup. In a companion paper, we have developed such asymptotic theory for the PCA approach, showing consistency under very mild technical assumptions. Since the theory behind this approach is rather technical with lengthy proofs, we have decided to publish this part separately. The main assumptions (Assumptions 1 and 2 in Hörmann and Jammoul (2020)) required are:

1. The noise vectors  $(u_t)$  are i.i.d. zero mean and independent of the signals  $(X_t)$ . The processes  $(u_{ti}: 1 \leq i \leq p)$  are Gaussian with absolutely summable auto-covariances.
2. (a) The process  $(X_t: t \geq 1)$  is zero mean and  $L^4$ - $m$ -approximable. (b) The curves  $X_t = (X_t(s): s \in [0, 1])$  define fourth order random processes (i.e.,  $\sup_{s \in [0, 1]} EX_1^4(s) \leq C_X < \infty$ ) with a continuous covariance kernel. (c)  $E \sup_{s \in [0, 1]} X_1^2(s) < \infty$ .

As we can see, these conditions allow to incorporate a certain degree of weak dependence in the noise components as well weak dependence between functional data. We refer to Hörmann and Kokoszka (2010) for background on  $L^p$ - $m$ -approximability. Under these general conditions we obtain results of the type

$$\sup_{1 \leq t \leq T} \sup_{1 \leq k \leq p} |X_t(s_k) - \hat{X}_t(s_k)| \rightarrow 0$$

in probability. For a more detailed exposition of the assumptions as well as the associated proofs we refer to Hörmann and Jammoul (2020).

## 4 Simulation experiments

In this section we investigate the performance of our method on simulated data examples and compare the results with common techniques such as spline smoothing and functional principal components. We have performed extensive simulation studies that can be separated roughly into two types: smooth data (Section 4.1) and data where the underlying signal is rough (Section 4.2). Please note that the following simulations were performed in R version 4.0.3.

### 4.1 Recovering smooth signals

In order to have a realistic data generating process, we chose to adapt some real data for our purposes. We consider bi-hourly measurements of particulate matter PM10 in

Graz from October 1st 2010 to March 31st 2011. Thus, we have 48 observations per day over the course of 182 days. To have control over the actual structure of the data, we generated synthetic curves by the following four steps: (1) transform the raw data to functional data; (2) create a bootstrap sample of size  $T$ ; (3) evaluate the resulting sample on a grid of intraday time points; (4) add noise as in (1.1). In Step (1) we chose to do a least squares fit using 21 cubic B-splines. Then  $T = 50, 100, 200, 500$  curves were obtained by the bootstrapping in Step (2). These curves are considered as our signals  $X_1(s), \dots, X_T(s)$ . The signals in turn were evaluated at  $p = 24, 48, 96$  equidistant points in  $[0, 1]$ , giving rise to  $X_t(\mathbf{s})$  (Step (3)). In the final step we generated  $y_t = X_t(\mathbf{s}) + u_t$  with  $u_t \stackrel{\text{i.i.d.}}{\sim} N_p(0, \Omega)$ . For  $\Omega$  we chose the covariance of a sample  $(\varepsilon_1, \dots, \varepsilon_p)'$  from the stationary AR(1) process  $\varepsilon_k = \theta\varepsilon_{k-1} + \xi_k$ , where  $(\xi_k)$  is white noise with zero mean and standard deviation  $\sigma$ . Altogether we show four parameter settings (S1–S4). These are listed in Table 1. We remark that under settings S1 and S2 the noise components are i.i.d.  $N(0, \sigma^2)$ . In S3 and S4 we take into account potential autocorrelation in the intraday noise, which we believe is a realistic assumption in many applications.

		$\sigma$		
		1	2	4
	0		S1	S2
$\theta$	0.4	S3		
	0.8	S4		

Table 1: Parameter settings for the noise.

Our goal is now to recover the  $X_t(\mathbf{s})$ . First we compare our proposed method with a B-spline (B) and penalized B-spline smoothing approach (PB). Since the actual signal in this simulation setting is already contained in a space spanned by B-splines, we consider in fact a setup which should be very much in favour of these competitors. The B-spline smooth was computed using  $p/3$  basis functions and methods from the `fda` package in R. When  $p = 48$  this yields a number which is comparable to the actual number of B-splines used to create the signal, otherwise it is bigger. This is in line with Wood (2017), who suggests using more basis functions than one believes necessary and then using a penalization approach to smooth the result. We use penalized B-splines with a roughness penalty of the form  $\int X''(s)^2 ds$ . The penalty is added to the regular least squares equation and weighted with a parameter  $\lambda$ , which needs to be chosen. This has been done using a GCV (generalized cross validation) technique as described in Ramsay et al. (2009).

Furthermore, we compare our approach to the functional principal components (FPC) approach as motivated in Staniswalis and Lee (1998). To this end, we have used the function `fpca.sc` from the `refund` package in R, which smooths the empirical covariance prior to obtaining an estimate for the functional scores and subsequently, the estimated signal. The number of principal components was automatically chosen to be large enough to explain 99% of the variance. Note that in this approach, the smoothing of the covariance operator is done via penalized splines, which is in line with a suggestion in Di et al. (2009). The number of basis functions we used in this smoothing is  $p/3$  as well. In

our exploration we found that increasing the number of splines in this function requires immense computational effort while giving little improvement.

For the factor analysis, we used two different approaches. First, we used the PCA driven approach, as described in Fan et al. (2013) and explained in our Section 3 (PCA). We used the package `POET` in `R` in order to obtain the described estimates for the factor scores and loadings. Second, we use a Maximum-Likelihood approach (ML) with the EM algorithm as described in Bai and Li (2012) and implemented in the package `cate`. As for choosing the number of factors, we used the BCV and ED methods, which we described in Section 2.4. Implementation of these methods can also be found in the package `cate`. Note that for this implementation, a maximum number of factors `rmax` to be considered can be given. In this instance, we have chosen `rmax = 23`. In classical factor analysis the goal is to find a concrete interpretation for the specific factors; thus, it is usually desirable to have a small number of factors whose influence is easily discernible. In our setting, there is no need for such interpretation. When it comes to estimating the common components, estimates tend to be robust to the overestimation of the dimension  $L$ , but sensitive to too small  $L$ , see for example Fan et al. (2013). This is intuitive, as a too small  $L$  will result in important information being excluded from the fit, whereas we only add potentially “insignificant” information if  $L$  is chosen too large. Thus, we decided to choose  $\hat{L} = \max(\hat{L}_{\text{BCV}}, \hat{L}_{\text{ED}})$ . Practically we experience that in most settings  $\hat{L}_{\text{BCV}} \geq \hat{L}_{\text{ED}}$ . Hence the results remain basically unchanged if  $\hat{L} = \hat{L}_{\text{BCV}}$  is used.

In order to evaluate the quality of the respective approaches we are interested in the error  $X_t(\mathbf{s}) - \hat{X}_t(\mathbf{s})$ . While for real data  $X_t(\mathbf{s})$  is not observable, the signals are known in our simulation setting and we can hence define

$$\text{SSE}^{\text{appr}} = \frac{1}{pT} \sum_{i=1}^p \sum_{t=1}^T (X_t(s_i) - \hat{X}_t(s_i))^2. \quad (4.10)$$

The results of our Monte Carlo study with 250 iterations can be found in Tables 2 and 3. Methods that produce the minimal  $\text{SSE}^{\text{appr}}$  in each instance are bold.

The most important observations are summarised below:

1. The factor model approach outperforms the B-splines largely when  $p$  is growing slower than  $T$ . For example, when  $p = 24$ ,  $T = 500$  then with setting S3 the  $\text{SSE}^{\text{appr}}$  produced by the B-splines and penalized B-splines are more than 20 times bigger compared to the PCA factor model approach. The penalized B-splines work best if  $p$  is very large and  $T$  is small. In this case the noise can be very well smoothed on a local level.
2. For the B-splines based approaches the  $\text{SSE}^{\text{appr}}$  doesn't decrease with growing sample size only with increasing  $p$ . Against our expectations, the FPC method doesn't improve in practice with increasing  $T$  either, though theoretically it should (see the results in Müller et al. (2006)). It seems that the eigenfunctions from the smoothed covariances are oversmoothing the data and then local features of the data cannot be accurately recovered. In contrast, for both factor model estimators  $\text{SSE}^{\text{appr}}$  decreases significantly with increasing  $T$  as well as increasing  $p$ .
3. The PCA approach gave better results than the MLE approach.

Dimensions		SSE <sup>appr</sup> ( $\sigma = 2$ )						SSE <sup>appr</sup> ( $\sigma = 4$ )					
$p$	$T$	$\hat{L}$	B	PB	FPC	ML	PCA	$\hat{L}$	B	PB	FPC	ML	PCA
24	50	8	39.50	41.76	39.45	22.07	<b>16.59</b>	7	43.07	45.62	42.58	31.64	<b>27.07</b>
24	100	11	39.55	42.11	39.94	15.02	<b>10.33</b>	9	42.61	45.85	42.14	25.04	<b>21.18</b>
24	200	14	39.79	42.39	39.82	11.16	<b>7.32</b>	11	43.54	47	42.85	22.63	<b>18.4</b>
24	500	18	39.07	41.51	39.95	6.07	<b>4.34</b>	13	43.30	47.44	42.91	19.28	<b>14.93</b>
48	50	12	6.87	6.92	14.32	7.09	<b>5.51</b>	10	10.68	<b>10.66</b>	16.95	15.34	14.12
48	100	21	6.74	6.75	14.40	3.02	<b>2.62</b>	13	10.83	10.9	17.21	11.70	<b>10.82</b>
48	200	21	6.76	6.77	13.91	2.14	<b>2.1</b>	16	10.77	10.91	16.85	9.82	<b>9.08</b>
48	500	22	6.77	6.79	14.06	1.99	<b>1.96</b>	21	10.80	11.01	16.82	8.05	<b>7.87</b>
96	50	16	1.33	<b>1.19</b>	6.91	2.95	2.69	12	5.24	<b>4.13</b>	9.14	9.88	9.67
96	100	21	1.32	<b>1.18</b>	7.02	1.72	1.68	16	5.24	<b>4.14</b>	9.03	7.08	6.96
96	200	22	1.32	<b>1.18</b>	7.21	1.32	1.33	19	5.24	<b>4.17</b>	9.00	5.53	5.42
96	500	22	1.32	1.18	7.16	1.10	<b>1.09</b>	21	5.24	<b>4.2</b>	8.78	4.30	4.34

Table 2: Simulation Results for the synthetic PM10 data with i.i.d noise

We have also experimented with further simulations settings. Not surprisingly, by further increasing  $\sigma$ , SSE<sup>appr</sup> increases for all methods. Nevertheless we observe that in comparison to each other the methods behave similarly as in the settings described. The combination large  $\sigma$ , large  $p$  and very small  $T$  (e.g.,  $T = 10$ ) favours our competitors, while our proposed approach improves considerably with growing  $T$  in all instances. For only mildly larger  $T$  and much larger  $p$  (e.g.,  $p = 96, 192$  and  $T = 30$ ) we immediately obtain estimates that are competitive with the other approaches. Since the signals in our simulations are relatively smooth, the good performance of smoothing methods is not surprising for large  $p$ . For curves with rough signal, smoothing approaches are not able to recover specific features of the signal due to oversmoothing. This phenomenon can be observed in the following simulation study.

Dimensions		SSE <sup>appr</sup> ( $\theta = 0.4$ )						SSE <sup>appr</sup> ( $\theta = 0.8$ )					
$p$	$T$	$\hat{L}$	B	PB	FPC	ML	PCA	$\hat{L}$	B	PB	FPC	ML	PCA
24	50	8	38.50	40.46	38.99	20.7	<b>14.61</b>	8	39.51	41.56	39.95	21.07	<b>15.15</b>
24	100	12	38.63	40.71	39.22	12.37	<b>7.34</b>	12	39.71	41.78	40.07	13.44	<b>8.51</b>
24	200	18	38.42	40.49	39.14	4.52	<b>2.88</b>	18	40.35	42.17	40.63	5.76	<b>4.19</b>
24	500	19	38.88	40.69	39.62	2.23	<b>1.63</b>	19	40.09	41.66	40.51	4.31	<b>3.47</b>
48	50	21	6.05	6.12	13.55	1.21	<b>1.08</b>	21	8.00	8.06	14.83	2.71	<b>2.66</b>
48	100	21	6.18	6.25	14.00	0.92	<b>0.91</b>	21	7.91	7.98	15.71	2.6	<b>2.58</b>
48	200	22	6.13	6.21	13.65	0.88	<b>0.87</b>	22	7.90	7.97	15.41	2.58	<b>2.56</b>
48	500	22	6.16	6.23	13.71	0.86	<b>0.85</b>	22	7.87	7.94	15.08	2.57	<b>2.56</b>
96	50	21	0.70	<b>0.69</b>	6.55	0.89	0.84	21	2.43	<b>2.42</b>	7.73	2.58	2.5
96	100	22	0.70	<b>0.69</b>	6.58	0.71	0.69	22	2.42	2.42	7.94	2.4	<b>2.36</b>
96	200	22	0.70	0.69	6.79	0.64	<b>0.62</b>	23	2.42	2.41	7.93	2.37	<b>2.32</b>
96	500	22	0.70	0.69	6.65	<b>0.56</b>	<b>0.56</b>	23	2.43	2.42	8.03	2.35	<b>2.29</b>

Table 3: Simulation Results for the synthetic PM10 data with AR(1) noise

## 4.2 Recovering rough signals

We have already stressed that the theory underlying competing methods depends heavily on the smoothness of the underlying curves. We check in the following simulation setting the practical impact of "rough" signals on the respective methods. More specifically, our  $X_t(s)$  are defined on  $[0, 1]$  and are constructed as follows:

$$X_t(s) = \sum_{k=1}^3 \xi_{tk} \varphi_k(s),$$

where  $\varphi_1(s) = \mathbf{1}_{\{s > 1/3\}}$ ,  $\varphi_2(s) = 4(0.2 - |s - 0.5|)\mathbf{1}_{\{s \in [1/3, 2/3]\}}$  and  $\varphi_3(s) = \cos 6\pi s$ . Here,  $\mathbf{1}_{\{s \in [a, b]\}}$  denotes the characteristic function, that is  $\mathbf{1}_{\{s \in [a, b]\}} = 1$  if  $s \in [a, b]$  and 0 otherwise. The associated scores are independent and normally distributed  $\xi_{tk} \sim N(0, 2^{-2(k-1)})$  for  $k = 1, 2, 3$ . The noisy observations are obtained via  $y_{ti} = X_t(s_i) + u_{ti}$ , where  $u_{ti} \stackrel{iid}{\sim} N(0, \sigma^2)$ . We consider equidistant observation points  $s_i = (i - 0.5)/p$  for  $i = 1, \dots, p$ . Thus, the signals may be disrupted at  $s = 1/3$  (through  $\varphi_1$ ), and have a peak in  $[1/3, 2/3]$  (through  $\varphi_2$ ). Figure 4 shows two sample curves (black line) and the corresponding noisy observations (circles).

We consider the configurations  $p = 20, 50, 70$  and  $T = 50, 100, 200, 400$  as well as  $\sigma^2 = 0.01, 0.05, 0.1$ . This gives rise to a total of 36 different settings, which have been repeated 200 times each. The signal is estimated by the methods PCA, PB and FPC. The rest of the procedure is the same as in Section 4.1. The results have been summarized for each configuration and approach in Table 4. We see that the factor model approach (PCA) nearly always outperforms its competitors. It is evident that the penalized B-spline as well as the FPCA approach both fail to accurately estimate the signal at the discontinuity  $s = 1/3$ . See Figures 4 and 5. The factor model approach on the other hand is entirely unperturbed by this discontinuity and outperforms its competitors in

many settings by a huge margin.

We also mention that  $\hat{L}$  can be overestimated as can be seen in the case of  $\sigma^2 = 0.01$ . Despite the mild overestimation of the required number of factors, we see no negative impact on the recovery of the signal.

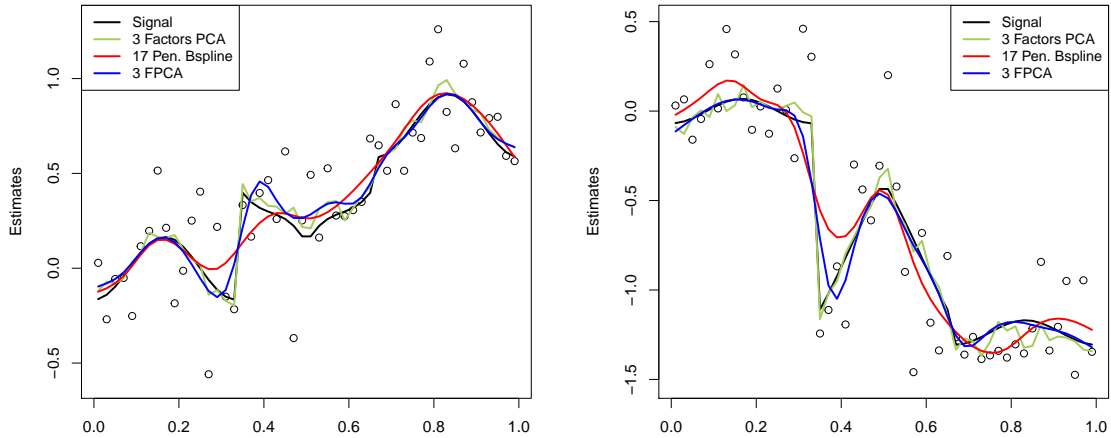


Figure 4: Estimates for the rough signal simulation for  $p = 50, T = 200, \sigma^2 = 0.05$ . Dots represent the noisy observations.

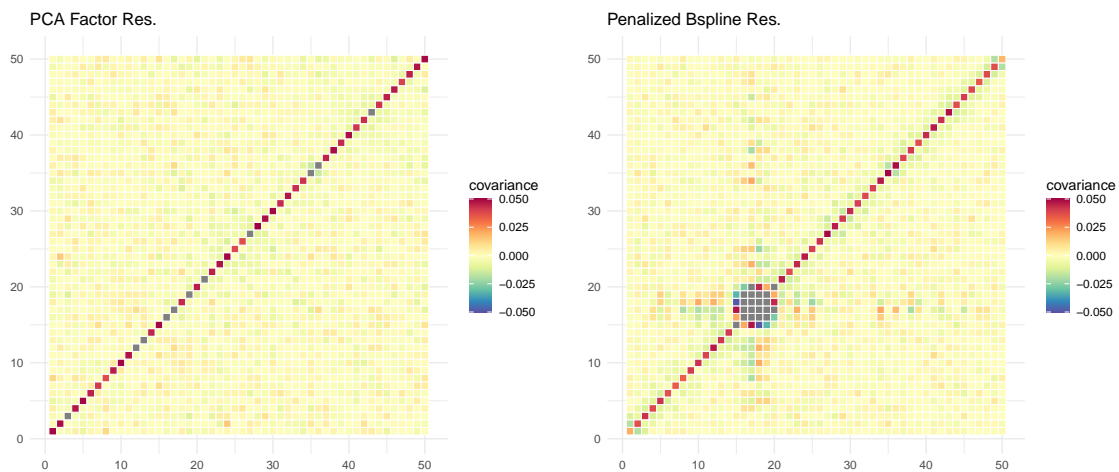


Figure 5: Heat map of the empirical covariance matrix of the residuals for the PCA (left) and PB approach (right) for the rough signal simulation.

Dimensions		SSE <sup>appr</sup> ( $\sigma^2 = 0.01$ )				SSE <sup>appr</sup> ( $\sigma^2 = 0.05$ )				SSE <sup>appr</sup> ( $\sigma^2 = 0.1$ )			
p	T	$\hat{L}$	PB	FPC	PCA	$\hat{L}$	PB	FPC	PCA	$\hat{L}$	PB	FPC	PCA
20	50	4	0.035	0.025	<b>0.004</b>	3	0.051	0.031	<b>0.012</b>	3	0.066	0.037	<b>0.026</b>
20	100	5	0.035	0.025	<b>0.003</b>	3	0.051	0.03	<b>0.01</b>	3	0.067	0.037	<b>0.02</b>
20	200	5	0.035	0.024	<b>0.003</b>	3	0.052	0.029	<b>0.009</b>	3	0.065	0.036	<b>0.018</b>
20	400	6	0.035	0.024	<b>0.003</b>	3	0.052	0.029	<b>0.009</b>	3	0.065	0.035	<b>0.016</b>
50	50	5	0.010	0.006	<b>0.003</b>	3	0.020	0.009	<b>0.007</b>	3	0.027	<b>0.013</b>	0.015
50	100	5	0.010	0.006	<b>0.002</b>	3	0.020	0.008	<b>0.005</b>	3	0.027	<b>0.011</b>	0.011
50	200	3	0.010	0.006	<b>0.001</b>	3	0.019	0.008	<b>0.004</b>	3	0.027	0.011	<b>0.008</b>
50	400	3	0.010	0.006	<b>0.001</b>	3	0.019	0.008	<b>0.004</b>	3	0.027	0.011	<b>0.007</b>
70	50	5	0.008	0.004	<b>0.002</b>	3	0.016	0.007	<b>0.006</b>	3	0.022	<b>0.01</b>	0.013
70	100	4	0.008	0.004	<b>0.001</b>	3	0.016	0.006	<b>0.004</b>	3	0.022	<b>0.008</b>	0.009
70	200	3	0.008	0.004	<b>0.001</b>	3	0.016	0.006	<b>0.003</b>	3	0.022	0.008	<b>0.007</b>
70	400	3	0.008	0.004	<b>0.001</b>	3	0.016	0.005	<b>0.003</b>	3	0.022	0.007	<b>0.005</b>

Table 4: Simulation results for the rough signal simulation with i.i.d. errors

## 5 Real data illustrations

In the following subsections we analyse daily temperature data from Canada. We analyse data for several years at several spatial locations. The daily data throughout a year are transformed into annual temperature curves. We fit factor models (PCA, ML) and give comparisons to the basis function and the FCPA approach. Ramsay et al. (2009) suggests to smooth this type of data with 65 Fourier basis functions and a penalization term. We follow this route and consider additionally a B-spline basis (also with 65 basis functions) and a roughness penalty of the form  $\int (f''(x))^2 dx$ . The tuning parameter controlling the size of the penalization term is chosen with generalized cross validation techniques as in Ramsay et al. (2009).

### 5.1 The Montreal Temperature Data

We examine the data `MontrealTemp` from the `fda` package, which we shortly discussed in the introduction. The data documents the daily temperatures measured in Montreal from the years 1961 to 1994. In Figure 6 we have plotted the data, which is visibly very noisy. We observe the typical seasonal shape. The goal is to separate a structural signal from unsystematic noise.

In this functional time series only one factor is selected by the BCV and ED approach. The corresponding estimates for the signal are shown in Figure 7 for the year 1993. The B-splines fit (orange) and the Fourier smooth (red) basically coincide. Also there is no visible difference between PCA (green) and ML (mint) factor estimates. While basis function estimates as well as the FPCA method (blue) try to mimic the very noisy data in a wiggly line, the factor model estimates have a simple parabolic structure (though the paths are rough). This is what we actually may expect, because the irregularities in the raw data are not structured and not cross-sectionally systematic. These particular

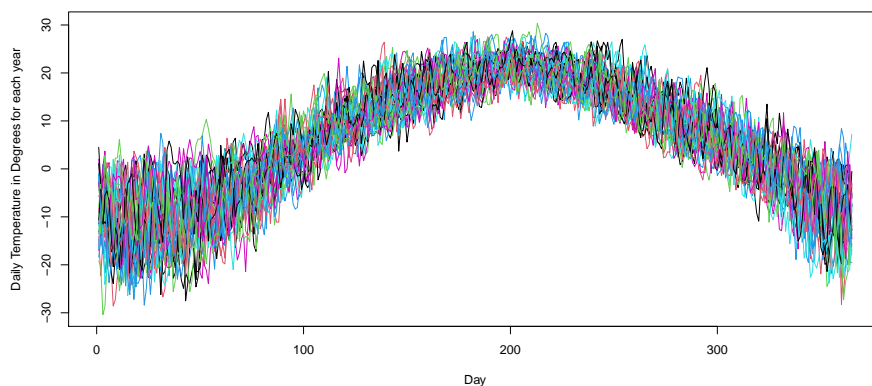


Figure 6: Yearly Montreal Temperature Data from 1961-1994.

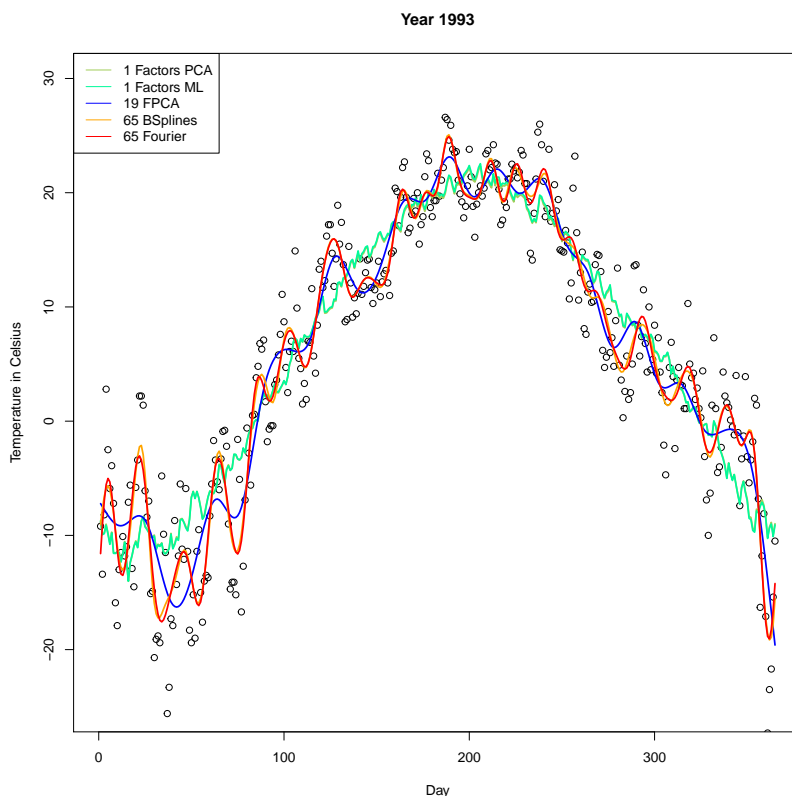


Figure 7: Montreal temperature curve for the year 1993. Dots represent daily raw data.

peaks and dips aren't part of the actual signal, but rather represent noise and random temperature fluctuations in each year.

When considering the lower left corner of the residual correlation matrices for the Fourier approach (see Figure 2), we see the banded structure of the related heat map.

This is also reflected in oscillating acf's (see again Figure 2). We obtained similar plots with the FPC method. Here the bands in the heatmap are broader and the oscillation in the acf is slower (see the plots on the left side in Figure 8). The factor PCA residuals appear more natural, and show a quickly decaying positive acf (plots to the right of Figure 8).

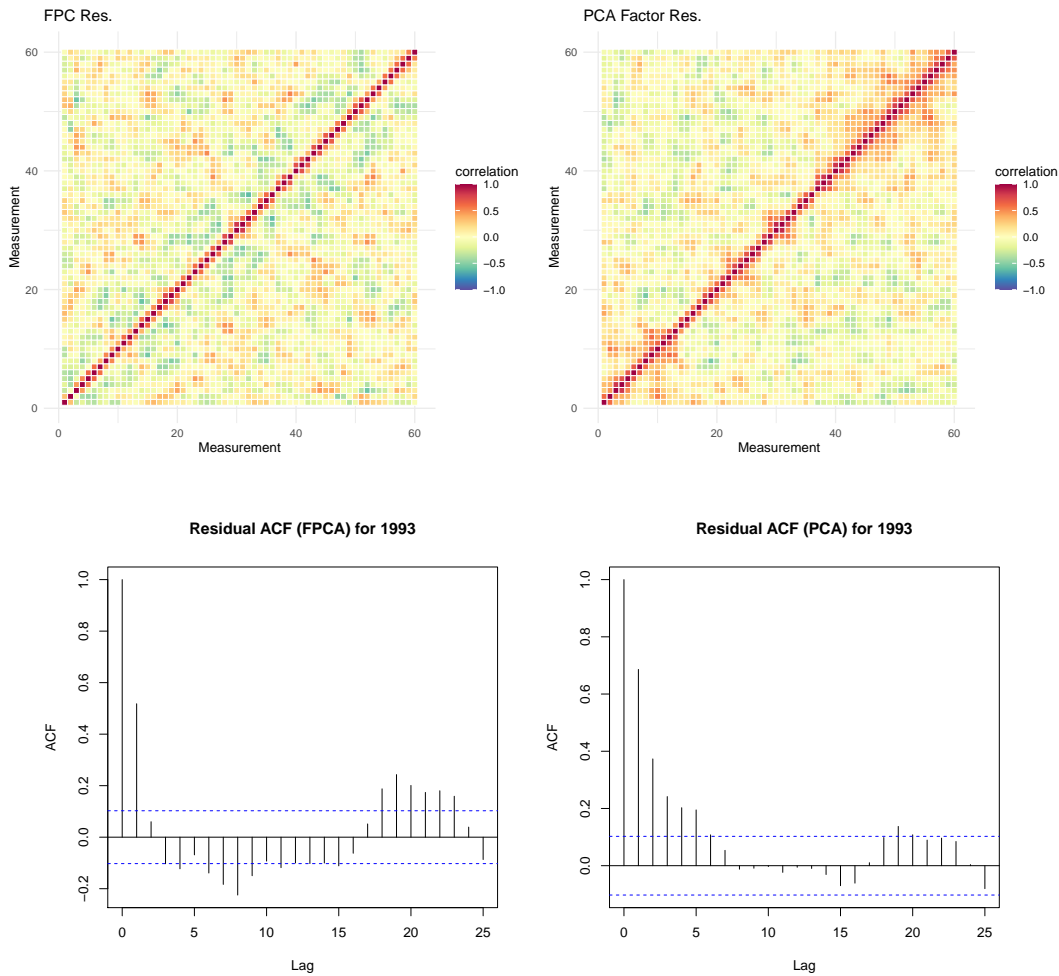


Figure 8: Heat maps of the empirical correlation matrices for the FPCA (top left) and PCA (top right) approach for the Montreal Data and associated estimated Residual ACF for the year 1993 for the FPCA (bottom left) and PCA (bottom right) approach.

## 5.2 The Canadian Weather Data

The data set `CanadianWeather` from the package `fda` is a popular toy dataset in the FDA community, see e.g., Ramsay et al. (2009). The full dataset includes daily measurements (in degrees Celsius) from 35 Canadian Weather stations averaged over the years 1960 to 1994. In Figure 9 we plot the corresponding raw data. Hence, these data compare well

to Section 5.1, only that here we have spatially instead of temporally collected functional data.

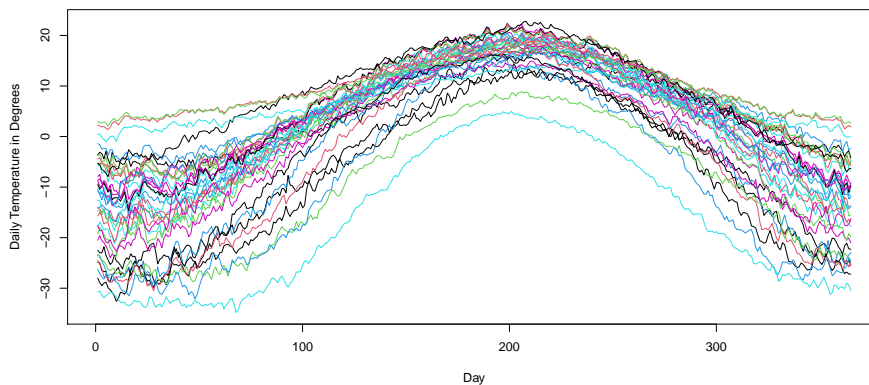


Figure 9: Plot of the raw Canadian Weather Data.

Since we again observed very little difference between the Fourier and the B-spline fit, and the PCA and ML estimates, respectively, we focus our attention on the Fourier smooth and the PCA method. Now that our sample consists of spatially distributed functional data and not of a functional time series, we expect that local peaks in the temperature curves are likely to be cross-sectionally correlated. Phases of too warm or too cold temperatures at one station are likely to occur also at other (typically closely located) stations and hence need to be attributed to a common signal. In fact, now our approach requires 13 factors and our estimated signal follows the raw data very closely. We show a part of two fitted curves in Figure 10. For the sake of better visibility, we have chosen to show only the first two months.

While the Fourier functions and the FPCA method appear attractive because of their smoothness, we see some spurious dependence in the residuals. Again, periodic behaviour remains visible in the acf for the basis functions approach. We see a very persistent positive acf for FPCA approach. Both indicate a problem with oversmoothing. We show the acf of the station Thunderbay in Figure 11 and remark that similar results can be observed in all other stations as well.

With the factor model approach there is a little positive correlation at lags 1 and 2 whereas for lags 3 or greater the acf does not significantly deviate from zero. In Figure 12 we show heat maps of the empirical correlation matrix of the residual vectors. Due to the big size of this matrix (this is a  $365 \times 365$  matrix) we display again the lower left  $60 \times 60$  sub-matrix related to the months January and February. A closer look reveals that the residuals from the Fourier fits yield alternating bands (parallel to the diagonal) of negative and positive correlation. This is in line with the oscillating acf's described earlier. We stress that we made the same observations when we used a penalized B-spline fit instead of the Fourier method. The FPCA approach results in a covariance which is far from diagonal and thus seems not appropriate for this data.

The two examples illustrate the sophistication of factor models particularly well, as

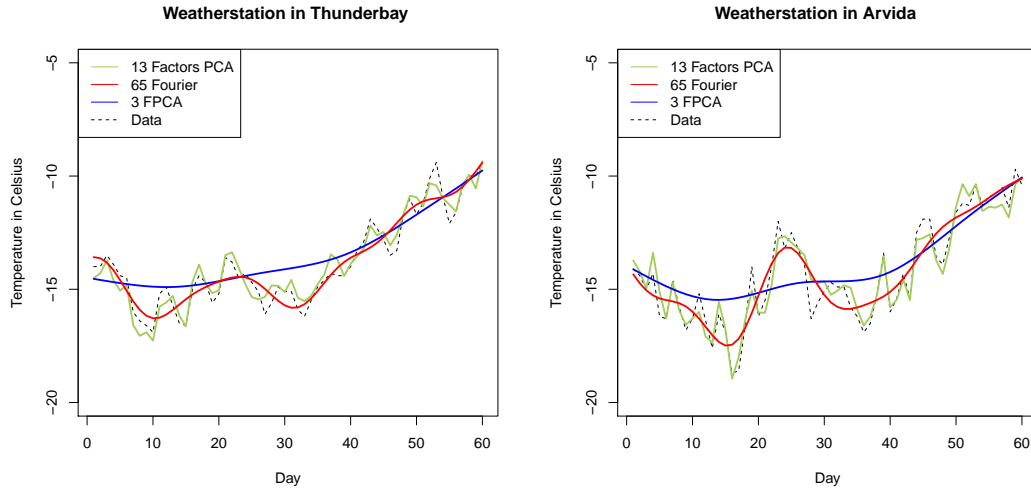


Figure 10: Average temperatures in two Canadian stations (Thunderbay and Arvida) in January and February.

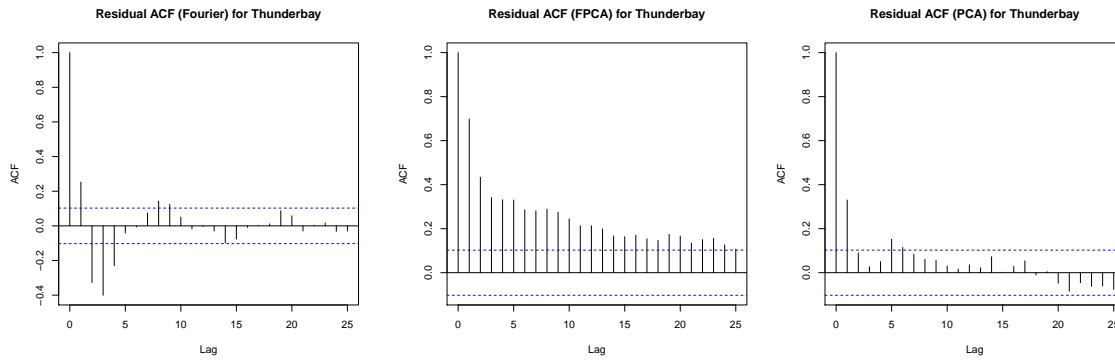


Figure 11: ACF of the residual vectors associated to the station Thunderbay for the Fourier (left) and FPCA (middle) and our PCA approach (right).

they truly manage to distinguish between systematic signal and noise in a very efficient way.

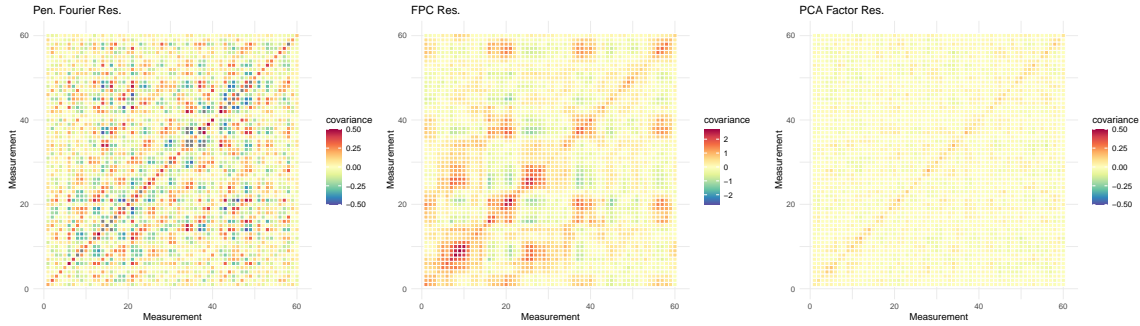


Figure 12: Heat map of the empirical correlation matrix of residuals for the Canadian Weather Data. For Fourier (left) and FPCA (middle) and our PCA approach (right).

## 6 Conclusion

In this paper we propose the use of factor models for estimating the underlying signals from raw measurement of discretely observed functional data. Using the Karhunen-Loève expansion, we show that a factor model structure is intrinsic in this type of data. Using annual temperature curves from Canada, we demonstrate that our method yields very plausible results. When compared to competing methods our approach is strongly supported by the residual diagnostics. We could also confirm in simulations on synthetic but realistic data that the performance of our proposed approach is very convincing. Furthermore, we show the far superior performance of our method when the signals are not smooth.

It is to be noted that the factor model approach doesn't yield curves, but produces discrete data. After consistently estimating the signal at observation points, we can use some suitable interpolation scheme to obtain functional data if required. For visualisation purposes we used simple linear interpolation in this paper. However, it needs to be stressed that in many numerical implementations we often *need* to work with discrete data. For example, in functional regression, we have to approximate  $\int b(s)X(s)ds$  by the Riemann sum  $\sum b(s_i)X(s_i)(s_{i+1} - s_i)$ , unless both  $b$  and  $X$  are given in a finite basis function expansion.

A theoretical foundation and rigorous investigation of the proposed method is left to a companion paper, see Hörmann and Jammoul (2020).

## Acknowledgement

We thank Jeff Goldsmith and Sonja Greven for a very helpful discussion on the `refund` package which we used to implement the FPCA method.

## References

- T.W. Anderson. *An Introduction to Multivariate Statistical Analysis*. Wiley, New York, 3 edition, 2003.
- J. Bai. Inferential theory for factor models of large dimensions. *Econometrica*, 71:135–171, 2003.
- J. Bai and K. Li. Statistical analysis of factor models of high dimension. *The Annals of Statistics*, 40:436–465, 2012. doi: 10.1214/11-AOS966.
- J. Bai and K. Li. Maximum likelihood estimation and inference for approximate factor models of high dimension. *The Review of Economics and Statistics*, 98:298–309, 2016.
- J. Bai and Y. Liao. Efficient estimation of approximate factor models via regularized maximum likelihood. *Journal of Econometrics*, 191:1–18, 2016.
- J. Bai and S. Ng. Determining the number of factors in approximate factor models. *Econometrica*, 70:191–221, 2002.
- D. Bosq. *Linear processes in function spaces: theory and applications*. Lecture Notes in Statistics. Springer, New York, 2000.
- G. Chamberlain and M. Rothschild. Arbitrage, factor structure, and mean-variance analysis on large asset markets. *Econometrica*, 51:1281–1304, 1983.
- I. Choi. Efficient estimation of factor models. *Econometric Theory*, 28:274–308, 2012.
- C.-Z. Di, C. Crainiceanu, B. Caffo, and N. Punjabi. Multilevel functional principal components. *The Annals of Applied Statistics*, 3(458–488), 2009.
- J. Fan, Y. Liao, and M. Mincheva. Large covariance estimation by thresholding principal orthogonal complements. *Journal of the Royal Statistical Society. Series B.*, 75, 09 2013.
- M. Forni and M. Lippi. The generalized dynamic factor model: representation theory. *Econometric Theory*, 17:1113–1141, 2001.
- M. Forni, L. Reichlin, M. Hallin, and M. Lippi. The generalized dynamic-factor model: Identification and estimation. *The Review of Economics and Statistics*, 82:540–554, 2000. doi: 10.1162/003465300559037.
- M. Forni, M. Hallin, Lippi M., and L. Reichlin. The generalized dynamic factor model: One-sided estimation and forecasting. *Journal of the American Statistical Association*, 100:830–840, 2005.
- P. Hall, H.-G. Müller, and J.-L. Wang. Properties of principal component methods for functional and longitudinal data. *The Annals of Statistics*, 34:1493–1517, 2006.

- M. Hallin and R. Liška. Determining the number of factors in the general dynamic factor model. *Journal of the American Statistical Association*, 102:603–617, 2007.
- S. Hörmann and F. Jammoul. Consistently recovering the signal from noisy functional data. *Preprint*, 2020.
- S. Hörmann and P. Kokoszka. Weakly dependent functional data. *The Annals of Statistics*, 38:1845–1884, 2010.
- L. Horváth and P. Kokoszka. *Inference for functional data with applications*. Springer Science and Business Media, 2012.
- H.-G. Müller, U. Stadtmüller, and F. Yao. Functional variance processes. *Journal of the American Statistical Association*, 101:1007–1018, 2006.
- E. Nadaraya. On estimating regression. *Theory of Probability & Its Applications*, 9: 141–142, 1964.
- A. Onatski. Determining the number of factors from empirical distribution of eigenvalues. *The Review of Economics and Statistics*, 92:1004–1016, 2010.
- A. Owen and J. Wang. Bi-cross-validation for factor analysis. *Statistical Science*, 31: 119–139, 2016.
- J. Ramsay, G. Hooker, and S. Graves. *Functional Data Analysis with R and MATLAB*. Springer, 1st edition, 2009.
- J.O. Ramsay and B.W. Silverman. *Functional Data Analysis*. Springer, New York, 2005.
- U. Stadtmüller and M. Zampiceni. *Stochastic Geometry, Spatial Statistics and Random Fields: Models and Algorithms*. Springer, Cham, 2015.
- J. Staniswalis and J. Lee. Nonparametric regression analysis of longitudinal data. *Journal of the American Statistical Association*, 93:1403–1418, 1998.
- J. Stock and M. Watson. Macroeconomic forecasting using diffusion indexes. *Journal of Business & Economic Statistics*, 20:147–162, 2002a.
- J. Stock and M. Watson. Forecasting using principal components from a large number of predictors. *Journal of the American Statistical Association*, 97:1167–1179, 2002b.
- M.P. Wand and M. C. Jones. *Kernel Smoothing*. Chapman & Hall, London, 1995.
- G. S. Watson. Smooth regression analysis. *Sankhyā, Series A (1961-2002)*, 26:359–372, 1964.
- S. Wood. *Generalized Additive Models: An Introduction with R*. Chapman and Hall/CRC, 2 edition, 2017.
- F. Yao, H.-G. Müller, and J.-L. Wang. Functional data analysis for sparse longitudinal data. *Journal of the American Statistical Association*, 100:577–590, 2005.